Efficiency Of Fabricated CNT-IPSF/Fe_3O_4 Nanocomposites In Removal Of Phenanthrenes From Contaminated Water

Shisia K. Silvanus, Naumih N., Nyambaka H, Andala D.M

Abstract: The increased demand for oil to supply the needs of industry and motorists has exposed the water sources to one of the greatest threats. The removal of selective organic pollutants such as phenanthrenes in aqueous solution was investigated by adsorption process on fabricated CNT-IPSF/Fe_3O_4 nanocomposites. Characterization of products confirmed the synthesis of individual nanomaterials in the nanocomposites. The SEM image of prepared CNTs showed configuration with abundant threadlike entities whose TEMs further confirmed evidence for formation of MWCNTs. The silica modified magnetite ($Fe_3O_4.SiO_2$) nanoparticles had clear, distinct and spherical shaped nanoparticles arranged in a 2-D closed packed manner. The XRD diffraction pattern showed well crystalline magnetite silica NPs with particle size 22.4 nm from the Debye-Scherrer equation. The SEM–EDAX analysis revealed large quantities of dispersive magnetite NPs with moderately uniform and cubic structures in the fabricated CNT-IPSF/Fe_3O_4 nanocomposites. Adsorption parameters were optimized at adsorbent dose (6 mg/20ml), contact time (40 mins), pH_{PZC} (4.5) and pH 5. Adsorption kinetics followed pseudo second order kinetics while the adsorption isotherm favored was Freundlich isotherms. The nanocomposites were not largely affected by of counter PAHs as its removal efficiency was 42.2 % and 40.8 % in the presence of naphthalene and anthracene respectively. This was replicated in its application in phenanthrenes removal from industrial wastewater in which the nanocomposites showed 63 % phenanthrenes removal. The trend for the studied desorption solvents was acetone > hexane > methanol which had 47 %, 42 % and 22 % removal efficiency respectively. The adsorption-desorption cycles involved a small volume of phenanthrene concentrates being recovered with gradual decrease in adsorption capacity for phenanthrene from 33.46 - 28.68 µg/g after three cycles. The desorption efficiency of phenanthrenes increased from to 49.81 to 56.98 wt.% implying that the developed nanocomposites could be advantageously be reused several times in removal of toxic phenanthrenes from industrial waste water.

Key words: Adsorption, characterization, Debye-Scherrer equation, fabricated, nanocomposites, phenanthrenes, wastewaters

1. INTRODUCTION

The outflow of urban and industrial wastewater contaminated with oil spills from petroleum and its derivatives is a chronic problem due to port activities [1]. Polycyclic aromatic hydrocarbons (PAHs) are one of the major groups of these organic contaminants [2] whose presence in drinking, surface and waste water has generated much public health concern [3, 4]. Polycyclic aromatic hydrocarbons have serious effects to man such as cataracts (anthracene), liver and kidney damage (phenanthrenes), and destruction of red blood cells (nanphthalene). As a result of their persistence in the environment, they have been classified as priority pollutants with well-established restrictive limits by most environmental regulatory agencies [5]. The increasingly stringent water quality standards, compounded by emerging contaminants, have brought new scrutiny to the existing water treatment methods [6].

- *Shisia K. Silvanus, Naumih N., Nyambaka H, Andala D.M*
- *Department of Chemistry, Kenyatta University, Nairobi, Kenya kuboka2003@gmail.com*
- *Department of Chemistry, Kenyatta University, Nairobi, Kenya nyambaka.hudson@ku.ac.ke*
- *School of Pharmacy and Health Sciences, United States International University, Nairobi, Kenya noah.naumih@ku.ac.ke*
- *Department of Chemistry, MultiMedia University, Nairobi, Kenya andalad@gmail.com*

Adsorption is affected by a number of factors especially contact time, initial PAHs concentration but to a lesser extent pH, water hardness and salinity [3, 7]. The experiment was then conducted under the optimized situations and resulting response was compared to that of standard activated carbon for its efficiency. This study was undertaken to investigate the application of the fabricated CNT-IPSF/Fe_3O_4 nanocomposites using carbon nanotubes infused polysulfone (CNT-IPSF) in the removal phenanthrenes from wastewater.

2. EXPERIMENTAL STAGE

2.1. Fabrication of CNT-IPSF/Fe_3O_4 nanocomposites

Carbon nanotubes were synthesized by method outlined in previous studies [8] and characterized by SEM and TEM techniques. Magnetite silica nanoparticles were prepared via solvothermal reaction [9] and characterized using SEM techniques. Structural and particle size were determined by X-ray diffractometer (Shimadzu, XRD-6000) equipped with CuKα radiation source using Ni as filter at setting of 30 kV/30 mA in the angular range $10 \leq 2\theta \leq 90^{o}$ with a scanning speed of 0.02°/s and a step time of 3s. The CNT-IPSF/Fe_3O_4 nanocomposites were characterized by SEM–EDAX technique and tested for removal of phenanthrenes from wastewater.

2.2 Testing efficiency of CNT-IPSF/Fe_3O_4 nanocomposites in removal of phenanthrenes

2.2.1 Chemicals

All chemicals used in this study (methanol and phenanthrenes) were of analytical grade (99 %, R&M Chemicals, UK). Working solutions from stock phenanthrenes (1000 µg/L) were prepared by further dilutions of the stock solutions in methanol. A set of standards of phenanthrene solution at the concentration of 5-100 µg l^{-1} was made in methanol and were stored at room temperature (26 ± 2°C). Phenanthrenes concentrations were quantified by UV–Visible Spectrophotometer (SpecordR 200 Plus) from absorbance of phenanthrenes at 293 nm. The adsorbed phenanthrenes concentration was determined from the standard calibration curves. Percentage phenanthrenes removal was also calculated.

2.2.2 Optimization of the adsorption parameters

2.2.2.1 Effect of Adsorbent Dose

20 ml aliquot solutions having initial concentration of 15 and 20 µg/L of the phenanthrene solutions was placed in conical flasks. Each of the masses (2 mg, 4 mg, 6 mg, 8 mg, 10 mg, and 20 mg) of the nanocomposites was added to each set of the conical flasks and agitated (120 rpm) for 60 min. The mixtures were filtered and the phenanthrene concentrations in the filtrates were determined by UV–Visible Spectrophotometer (SpecordR 200 Plus). All the experiments involved 10 samples.

2.2.2.2 Effect of Contact Time

The adsorption studies were carried out by adding 6 mg of nanocomposite into conical flasks each containing 20 ml for 15 and 20 µg/L phenanthrene solutions. Each set of the mixtures were agitated and aliquots of the filtrates from the conical flasks drawn after 5, 10, 20, 30, 40 and 60 min of agitation time. Amounts of phenanthrenes in the aliquots were quantified with UV–Vis Spectrophotometer (Specord^R 200 Plus) where absorbance of residual phenanthrenes in filtrates was recorded at 293 nm as per literature [10]. All the experiments were carried out on 10 samples.

2.2.2.3 Effect of pH on Phenanthrene Adsorption

The pH_{pzc} value was determined using the solid addition method [11]. A series of experiments, with 20 ml aliquots of 15 and 20 µg/L phenanthrene solutions in conical flasks were conducted under different pH (1, 4, 7, 8 and 12) to investigate the effect of pH on the phenanthrenes adsorption. The pH was first adjusted to a designed value with 0.1 M HNO_3 or 0.1 M NaOH. About 6 mg of the nanocomposite was added to each flask and agitated in a shaker (120 rpm) for 60 minutes at 25 ^oC. The suspensions were filtered and the concentration of phenanthrene in the filtrates was determined using UV–Vis Spectrophotometer (Specord^R 200 Plus).

2.2.3 Determining Adsorption Kinetics Model for Phenanthrene Adsorption onto Adsorbent

The kinetics on the adsorption was carried out in continuously stirred conical flasks each containing 6 mg of nanocomposite in 20 ml of 20 µg/L phenanthrene solutions at 25 ^oC. Ten experiments involved the use of two 20 ml portions of 20 µg/L of phenanthrene solutions in which one portion was treated with 6 mg of the nanocomposites while the other portion was treated with 6 mg of activated carbon standard adsorbent (control) at different adsorptions times of 5, 10, 20, 30, 40 and 60 min and analyzed for residual phenanthrene concentration by UV-Vis spectrometry at 293 nm (Specord^R 200 Plus). The adsorption data obtained were fitted to adsorption kinetic models.

2.2.4 Determining Adsorption Isotherm Model for Phenanthrene Adsorption onto Adsorbent

The initial concentration of the phenanthrene was varied between 1 and 10 µg/L. A known weight (6 mg) of the nanocomposites was shaken with 20 ml of phenanthrene standards at pH 5 for 60 mins (optimized contact time) at 25 ^oC on a rotatory shaker to ensure removal equilibrium was reached. The nanocomposite was removed after centrifugation (10 min) for easy filtration and the residual phenanthrenes concentrations were determined by UV-Vis spectrophotometer. All of the adsorption experiments were conducted in triplicate, and the average results are reported. For control experiments, 6 mg of activated carbon (standard adsorbent) was put into plastic bottles with 20 ml of 1, 2, 4, 6, 8 and 10 µg/L of phenanthrene solutions at 25 ^oC and pH 5, and mixture shaken for 60 minutes of contact time. The mixtures were treated in similar way and residual phenanthrene determined by UV-Vis spectrophotometer. The adsorption data obtained were fitted to adsorption isotherms models.

2.2.5 Effect of Similar PAHs on Phenanthrene Adsorption

This was studied by using 6 mg nanocomposites in 20 ml portions of 20 µg/L phenanthrenes solutions each spiked with counter PAHs (naphthalene and anthracene) of concentrations 1.0 µg/L. Further, control experiments involved putting 6 mg of activated carbon adsorbents into six conical flasks with each 20 ml portions having 20 µg/L phenanthrene solutions spiked with 1.0 µg/L concentrations of naphthalene and anthracene.

2.3 Application of CNT-IPSF/Fe_3O_4 Nanocomposite in Wastewater Treatment

2.3.1 Wastewater Sampling

Ten water samples containing industrial effluents of about one litre capacity were collected using a standard sampling technique [12]. Care was taken to avoid contamination of the sample during sampling, handling and transport to the laboratory by using glass containers for phenanthrenes as leaching and adsorption are minimal. Sample containers were cleaned and where reagents were added during the preservation step, a sample of the added reagents was also submitted for analysis as a reagent blank. The samples were immediately cooled (on ice) before further analysis.

2.3.2 Wastewater Treatment

Prior to sorption and desorption experiments, the water samples were filtered and portions of it analyzed for initial phenanthrenes concentrations using UV-Vis spectrometer. The rest of water samples were stored at 4 ^oC in a refrigerator for further analysis. 20 mL each of the water

samples was gently agitated with 6 mg of CNT-IPSF/Fe_3O_4 nanocomposites and activated carbon adsorbent separately on a rotatory shaker (120 rpm) for 1 h at 25 ^oC. Before UV-Vis analysis, the mixtures were immediately filtered through No 1 paper filter. The adsorbents with adsorbed phenanthrene were washed three times using acetone. All the experiments were carried out on 10 samples.

2.4 Regeneration and Reusability of the CNT-IPSF/F_3O_4 Nanocomposites using Phenanthrenes

2.4.1 Adsorption-Desorption Experiments

Each of the 6 mg nanocomposites was continuously stirred with 20 µg/L phenanthrene solutions (20 ml) in conical flasks to allow adsorption to take place. Upon filtration, each adsorbent with phenanthrene load was transferred to each conical flask containing 20 ml desorption solvents of methanol, n-hexane and acetone. The mixtures were shaken at 120 rpm for 18 h followed by determination of the concentration of phenanthrene in the filtrates after desorption. Control experiments involved putting 6 mg of standard activated carbon adsorbent into each of the conical flasks (pools) containing 20 µg/L phenanthrene solutions, agitating at 120 rpm for 18 hours. The phenanthrenes in filtrates after washing spent adsorbent with phenanthrene load with methanol, n-hexane and acetone was determined by UV-Vis spectrometer.

2.4.2 Reusability of CNT-IPSF/Fe_3O_4 Nanocomposites

To investigate the reusability of the nanocomposites, desorption and regeneration of phenanthrene-loaded CNT-IPSF nanocomposites were carried out. After adsorption process the adsorbent was separated and washed several times with methanol to remove any unadsorbed phenanthrenes. Desorption studies were performed by mixing resultant phenanthrene-loaded adsorbent with 20 mL of acetone in water shaker bath for 1h, filtered and the adsorbent was dried. The dried phenanthrene-loaded adsorbent was mixed with 20 mL of fresh acetone, shaken (1h) and separated from the solution followed by drying. The process was repeated three times to investigate reliability of the adsorption test for possible reuse of the adsorbent as per the equation (1):

$$\%\ \text{Desorption Efficiency} = \frac{\text{Amount of metal ions desorbed}}{\text{Amount of metal ions adsorbed}}\ x\ 100 \quad \text{.. (1)}$$

3. RESULTS

3.1. Characterization of CNT-IPSF/Fe_3O_4 Nanocomposites

The SEM image of prepared CNTs (Fig. 1a) depicts a configuration with abundant threadlike entities. The TEM image further provides evidence that the twisting and winding entities confirming formation of MWNTs (Fig. 1b). From the SEM micrograph of the silica coated magnetite (Fe_3O_4.SiO_2) nanoparticles (Fig. 1c), it was found that clear and distinct spherical shaped particles were obtained with addition of TEOS content. The monodispersed nanoparticles were arranged in a 2-D closed packed manner, demonstrating the uniformity in the nanoparticle size. Due to their nanoscale measurements,these NPs could be well suited for many applications involving its incorporation in nanocomposites fabrication. The diffraction pattern (Fig. 1d) showed that the synthesized magnetite silica NPs are well crystalline, and the position and the relative intensity of the diffraction peaks matched well with the standard XRD data (JCPDS file No. 19-0629) [13]. Fitting the XRD data to Gaussian and Lorentz line profile (not shown here), two patterns were obtained in which particle size was determined as 22.4 nm from the Debye-Scherrer equation (2):

$$T = \frac{C\lambda}{B\cos\theta} = \frac{C\lambda}{(B_{sp}^2 - B_{St}^2)^{\frac{1}{2}}\cos\theta} \quad \text{..... (2)}$$

The structure of the nanocomposites was characterized by SEM–EDAX technique (Fig. 2a) in which large quantities of dispersive magnetite silica nanoparticles have moderately uniform and cubic structures. The cylindrical needle-like threads of CNTs can be seen interlinking with the silica coated magnetite NPs (Fig.2a). The SEM of as-prepared CNT/Fe_3O_4 nanocomposites revealed well packed and uniform structure with higher surface area suitable for adsorption studies. In this study, carbon nanotubes (CNTs) were sonicated with magnetite NPs which altered their mechanical properties through thorough mixing. In addition, such process also increases the number of defects on the walls of the CNTs; breaking inertness and enhancing reactivity [14]. Chemical analysis from EDS (Fig. 2b) confirms the presence of Fe and O elements. With the stoichiometry Fe_3O_4 phase, the presence of C and S confirms the inclusion of CNTs and infused polysulfone respectively.

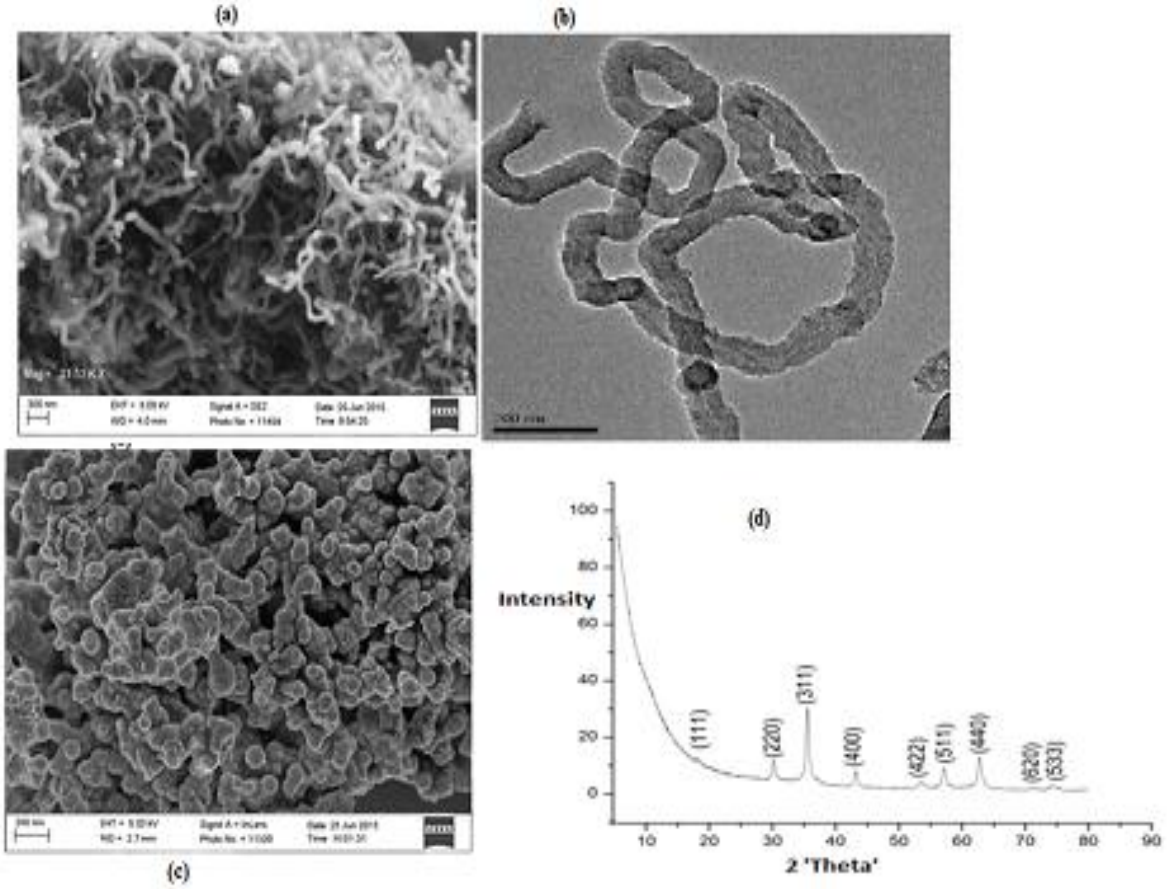

Fig. 1 Characterization of products

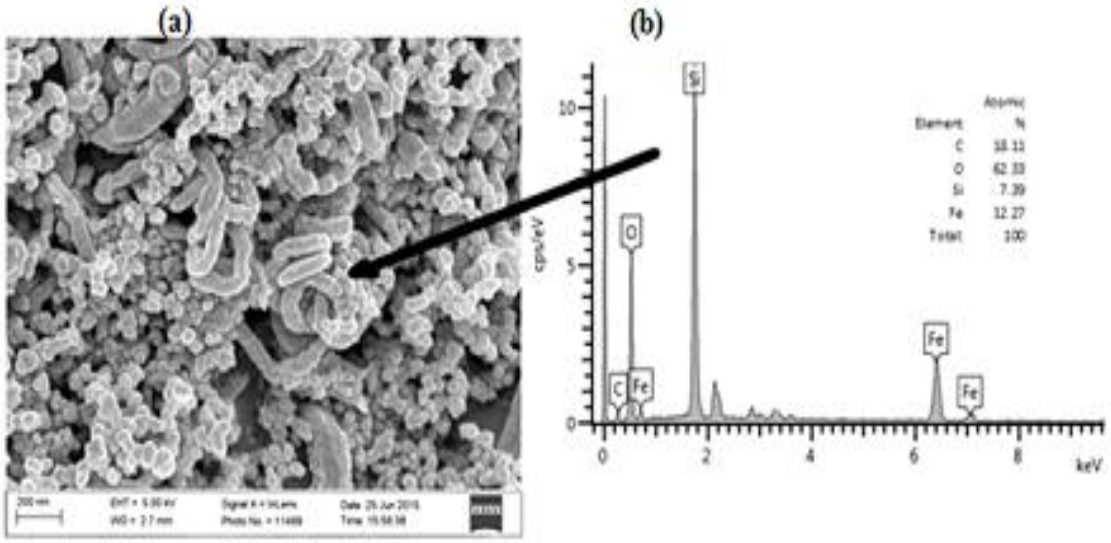

Fig. 2 SEM-EDAX analyses for CNT-IPSF/Fe_3O_4 nanocomposites

3.2 Efficiency of CNT-IPSF/Fe_3O_4 Nanocomposite in Removal of Phenanthrenes from Wastewater

3.2.1 Optimization of Factors

From the pH_{pzc} curve of the sample, the pH_{pzc} value was found to be around 4.5 (Fig. 3a) revealing possible presence of acidic oxygen-bearing surface functionalities, such as -COOH and -OH groups. The % phenanthrenes removal increased from 28 – 45 % and 23 – 48 % for initial phenanthene concentration of 20 and 15 µg/L respectively. The initial rapid increase reaching optimum at about 6 mg adsorbent observed (Fig. 3b) could be due to the increased availability of binding sites and surface area for easy adsorption of phenanthrenes [15]. The results show a sharp increase in phenanthrenes removal between 10-20 minutes of contact time from 43 – 49 % and 34 – 41 % for both 20 and 15 µg/L respectively (Fig. 3c). This could be attributed to the fact that a large number of vacant surface sites were available for adsorption during the initial stage, and with lapse of time, the remaining vacant sites would continually reduce [16]. Adsorption equilibrium was attained approximately within 40 min of contact time with adsorbent. The phenanthrene adsorption efficiency gradually increased when the pH increased from 4 to 8 for both initial phenanthrenes concentration but 15 µg/L phenanthrenes showed sharp increase from 22 µg/g to 25 µg/g which corresponds to 14 % increase in phenanthrenes(Fig. 3d). The results demonstrate that the phenanthrene removal was mainly dependent on the possible π-π interactions between the adsorbent and phenanthrenes molecules.

3.2.2 Adsorption Kinetics Model for Phenanthrene Adsorption

The experimental values for adsorption of phenanthrenes involved agitating 6 mg/20 mL prepared (CNT-IPSF/Fe_3O_4) and standard (activated carbon) adsorbents in 20 µg/ L phenanthrenes concentrations, contact times 5-60 mins and pH5. In this study, two kinetic models were studied to describe the kinetics of adsorption. These included Pseudo First Order (equation 3; Fig. 4a) and Pseudo Second order (equation 4; Fig. 4b) [17].

$$log(Qe - Qt) = logQe - \frac{K_{1p}}{2.303}t \quad \text{..... (3)}$$

$$\frac{t}{Q_t} = \frac{1}{K_{2p}Q_e^2} + \frac{1}{Q_e t} \quad \text{..... (4)}$$

The kinetic parameters are shown in Table (1):

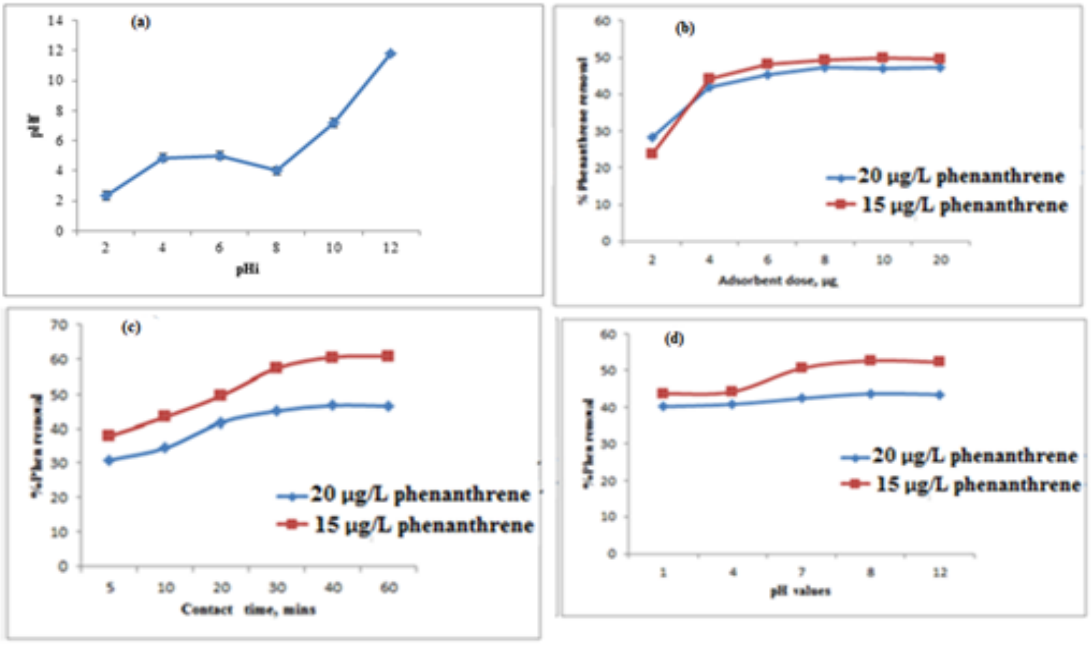

Fig. 3 Opimization factors (a) pHpzc (b) adsorbent dose (c) contact time (d) pH on CNT-IPSF/Fe3O4

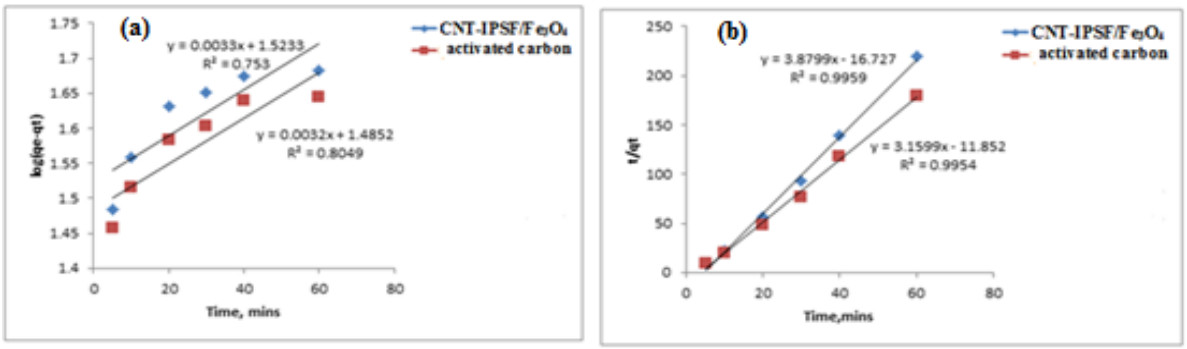

Fig. 4 Pseudo (a) 1st order and (b) 2nd order kinetics for phenanthrenes adsorptions

Table 1 Pseudo 1st order and 2nd order kinetic constants of CNT-IPSF/Fe3O4 and activated carbon

Kinetics		Parameters	Adsorbents	
			$CNT\text{-}IPSF/Fe_3O_4$	activated carbon
Pseudo order	1st	q_e	33.37	30.56
		$K_{1\rho}$	0.0076	0.0074
		R^2	0.753	0.8049
Pseudo Order	2nd	q_e	0.26	0.32
		$K_{2\rho}$	0.89	0.84
		R^2	0.9959	0.9954

From the above results, the adsorption kinetics followed the pseudo-second-order model. This model gives the best- fit to experimental data for phenanthrene for the prepared nanocomposites and standard activated carbon adsorbents studied in this work, which have highest correlation coefficient values of 0.9959 and 0.9954 respectively. This implied that the rate of occupation of adsorption sites is proportional to the square number of unoccupied sites, because the pseudo-second order model is based on a second order mechanism [18].

3.2.3 Adsorption Isotherm Modeling for Phenanthrene Adsorption

The initial phenanthrenes concentration provides an important force to overcome all mass transfer resistances of the target pollutant between aqueous and solid phase [19]. The subsequent removal of phenanthrenes using a constant amount of nanocomposites was examined at various concentrations in the range 1–10 µg/L. The adsorption isotherms data were fitted to both the Langmuir (equation 5; Fig. 5a) and Freundlich (equation 6; Fig. 5b) isotherm equations [20].

$$\frac{C_e}{q_e} = \frac{1}{q_m.b} + \frac{C_e}{q_m} \quad \text{..... (5)}$$

$$logq_e = logK_f + \frac{1}{n} logC_e \quad \text{..... (6)}$$

According to the R^2 for each sample in Table (2), the results show that the adsorption process could be described well with both Freundlich and Langmuir isotherms. Although both isotherms described the adsorption process very well, Freundlich isotherm, for each sample of the adsorbent fitted the behaviour better with higher correlation coefficient (>0.95) recorded for each sample suggesting multi-layer adsorption nature of the phenanthrenes on the CNT-IPSF/Fe_3O_4 adsorbent (Uddin et al., 2007). The values of n=1.5 is greater than 1, indicating the physisorption is much more possible. The obtained values for 1/n=0.66 is less than unity which is an indication that significant adsorption takes place for low phenanthrene concentrations.

3.2.4 Effect of Counter PAHs on Phenanthrene Adsorption

The effect of similar PAHs on adsorption was studied and the results are shown in Fig. 6. It can be seen that 1 µg/L of anthracene greatly reduced phenanthrene removal by a significant drop of about 1.27 and 1.10 % for both nanocomposites and activated carbon adsorbents respectively.

3.3 Industrial Wastewater Treatment for Phenanthrenes Removal

Application studies using real industrial wastewater was carried out to determine the practicality of the CNT-IPSF/Fe_3O_4 nanocomposites at optimum batch condition as shown in Fig. 7.

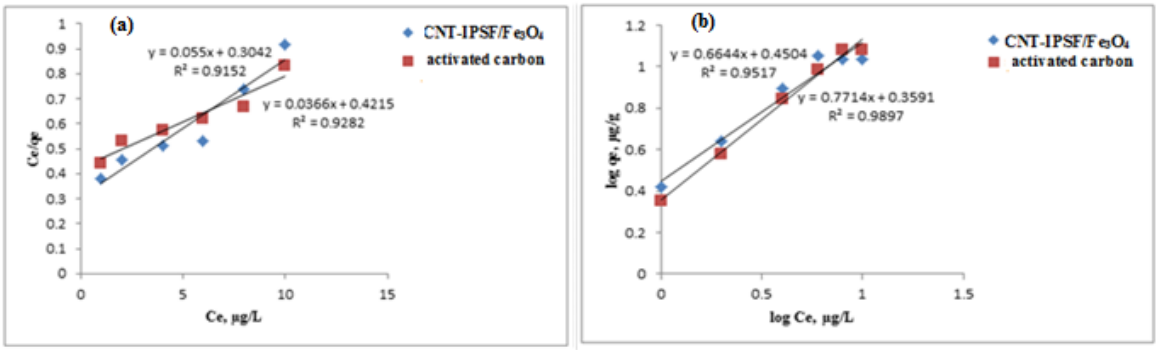

Fig. 5 (a) Langmuir and (b) Freundlich isotherm for phenanthrenes adsorptions

Table 2. Langmuir and Freundlich isotherm constants for phenanthrenes adsorption on CNT-IPSF/Fe3O4 nanocomposites

Isotherms	Parameters	adsorbents	
		CNT-IPSF/Fe_3O_4	activated carbon
Langmuir	Q_m	18.182	28.329
	b	0.1808	0.0868
	R^2	0.9152	0.9282
Freundlich	Kf	2.8210	2.2861
	1/n	0.6644	0.7714
	n	1.5051	1.2963
	R^2	0.9517	0.9897

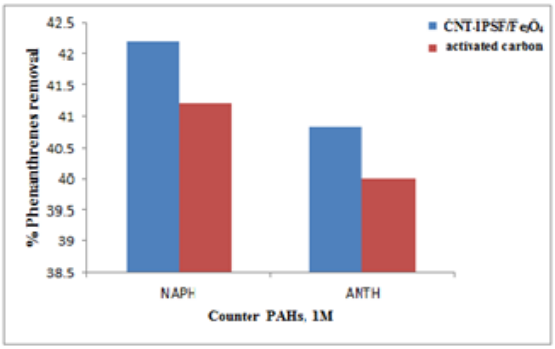

Fig. 6 Adsorption efficiencies of CNT-IPSF/Fe3O4 and activated carbon for phenanthrene in presence of other PAHs

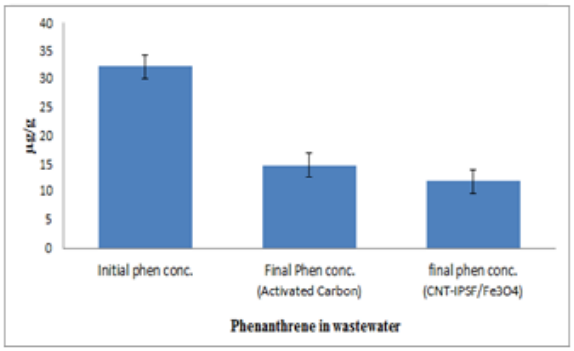

Fig. 7 Pb(II) ions removal from wastewater by CNT-IPSF/Fe_3O_4 and activated carbon

The prepared CNT-IPSF/Fe_3O_4 nanocomposites had about 63 % phenanthrenes removal as compared to 54 % for activated carbon adsorbent implying that the CNT-IPSF/Fe_3O_4 nanocomposites exhibited good adsorption performance for the treatment of wastewater samples. This observation may be due to attributed to the pi–pi electron interaction between the CNT-IPSF/Fe_3O_4 nanocomposites and phenanthrene molecules [21]. Since these molecules are not chemically bonded to atoms of the adsorbents, the aromatic core of the adsorbed phenanthrene molecules will exhibit stronger pπ–pπ interaction with the free surface of the adsorbent [22]. The prepared CNT-IPSF/Fe_3O_4 nanocomposite was therefore effective in removal of phenanthrene from industry wastewater.

3.4 Regeneration and Reusability Studies on Adsorbent Using Phenanthrenes

3.4.1 Adsorption-Desorption Studies

Fig. 8 compares removal efficiencies of methanol, n-hexane and acetone solvents for phenanthrene from CNT-IPSF/Fe_3O_4 and activated carbon adsorbents. The trend for the studied desorption solvents is acetone > hexane > methanol which may be explained on the basis of non-polarity, except for methanol which is most polar with polarity index value of 5.1 [3] exhibiting least desorption ability. This observation might likely be linked to the presence of different functional groups in acetone and methanol, and their associated interactions with the adsorbents. Acetone had the highest percentage removal for phenanthrene of 47.12 and 43.91 % for the nanocomposites and activated carbon adsorbents respectively. Hence, acetone which is ketone (R-CO-R) will likely interact more with the adsorbate than methanol which is an alcohol (R-OH).

3.4.2 Reusability of CNT-IPSF/Fe_3O_4 Nanocomposite for Phenanthrene

Adsorption-desorption studies were then carried out as a function of acetone solution on prepared CNT-IPSF/Fe_3O_4 nanocomposites to determine the reliability of the nanocomposites in reusability. In each adsorption-desorption cycle, a small volume of phenanthrene concentrates were produced (Fig. 9) implying no damage to the capacity of the nanocomposites. There was gradual decrease in adsorption capacity for phenanthrenes from 33.46 - 28.68 µg/g after three cycles showing good removal efficiency. This implied that the developed adsorbent could be advantageously be reused several times using acetone which is cheap, hence a very big comparative cost advantage over other common adsorbents for PAHs. In Fig. 10, the desorption efficiency of phenanthrenes increased from 49.81 to 56.98 wt %. This shows that the elution agent was efficient in desorbing the phenanthrenes from the nanocomposites. The lower removal efficiency could be due to the small unavoidable loss of adsorbent weight during desorption process [23].

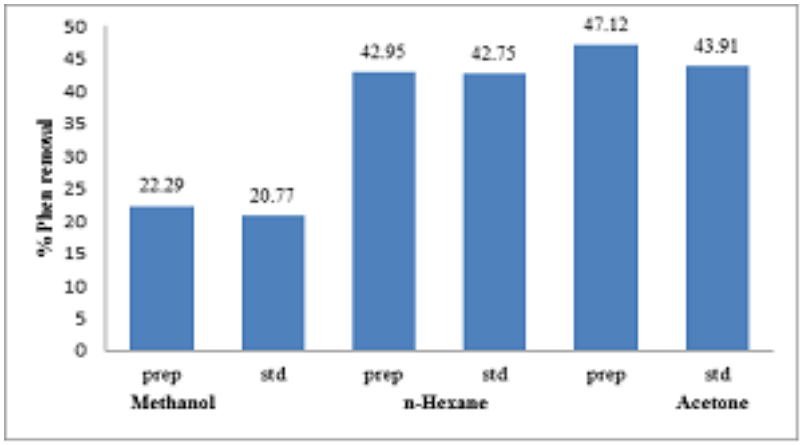

Fig. 8 Removal efficiency of different desorption solvents for phenanthrenes from adsorbents

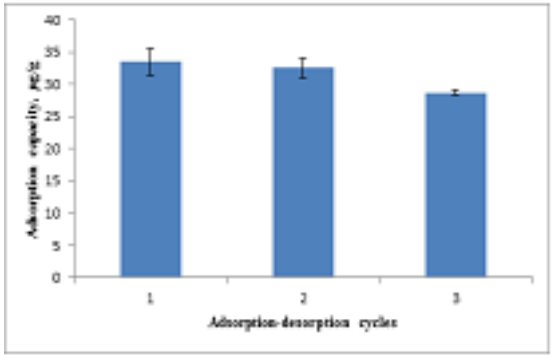

Fig. 9 Adsorption-desorption cycles

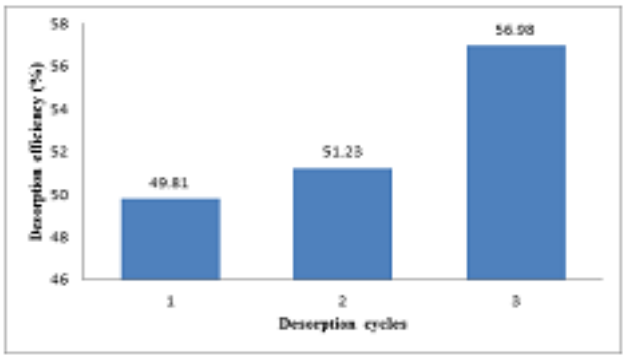

Fig. 10 Investigating the reliability of the desorption test

4. CONCLUSIONS

The CNT-IPSF/Fe_3O_4 nanocomposites were successfully fabricated from CNT-IPSF polymer and SiO_2·Fe_3O_4 nanoparticles based on various characterization procedures. The synthesized CNTs exhibited threadlike twisting and winding entities for multiwalled CNTs with average internal diameters of 40-50 nm from SEM characterization which was further confirmed by the TEM. The SEM image for the magnetite-silica formed revealed nanoparticles which were distinct and spherical. XRD analysis for magnetite silica NPs has very intense peaks, indexed as planes (220), (311), (400), (422), (511) and (440) which corresponds to a cubic spinel structure with crystal sizes of 22.4 nm from the strongest reflection of the (311) peak, using the Scherrer approximation (JCPDS No. 82-1533). The SEM for fabricated CNT-IPSF /Fe_3O_4 nanocomposite further revealed well packed and uniform structure depicting higher surface area suitable in adsorption studies. Chemical analysis spectrum from EDAX confirmed the presence of Fe, Si and O elements, with a stoichiometry Fe_3O_4 phase while C and S are candidates for CNTs and Infused polysulfone (IPSF) respectively. In this work, the use of CNT-IPSF/Fe_3O_4 nanocomposites for the removal of phenanthrenes from simulated drinking water showed a high removal capacity. The maximum adsorption capacities of the CNT-IPSF/Fe_3O_4 nanocomposites for phenanthrenes were found to be 63 % compared to 54 % for activated carbon used as a standard adsorbent. The equilibrium data obtained showed the best fit for the Freundlich isotherms with second order kinetic model for its adsorptions.

5. RECOMMENDATIONS AND FURTHER WORK

The fabricated CNT-IPSF/Fe_3O_4 nanocomposites material has capability for use in removal of phenanthrenes due to their good adsorption capacity, as well as ease of synthesis at relatively low cost. Further investigations should be done on the use of this nanocomposite material on adsorption of other PAHs. There will be need to carry out further investigations into the environmental side effects that may emanate from disposal of these nanomaterials since both health and environmental effects are not yet well researched areas. The nanocomposites should be characterized BET analysis in terms of its physical properties, such as surface area, pore volume and pore sizes that may influence the sorption capacity.

6. ACKNOWLEDGMENTS

We wish to thank the National Council of Science, Technology and Innovations (NACOSTI-Kenya) and Laikipia University, Kenya for generously supporting this research study. The authors acknowledge the contribution of the Technical staff in the Department of Chemistry, Kenyatta University, Kenya for guidance and availability of materials.

[1] REFERENCES

Tavakoly Sany, S., et al., Polycyclic aromatic hydrocarbons in coastal sediment of Klang Strait, Malaysia: distribution pattern, risk assessment and sources. PloS one, 2014. 9: p. e94907.

[2] Haritash, A. and C. Kaushik, Biodegradation aspects of polycyclic aromatic hydrocarbons (PAHs): a review. Journal of hazardous materials, 2009. 169(1): p. 1-15.

[3] Okoli, C.P., et al., Aqueous scavenging of polycyclic aromatic hydrocarbons using epichlorohydrin, 1, 6-hexamethylene diisocyanate and 4, 4-methylene diphenyl diisocyanate modified starch: Pollution remediation approach. Arabian Journal of Chemistry, 2015.

[4] Steingraber, S., Living downstream: An ecologist's personal investigation of cancer and the environment2010: Da Capo Press.

[5] Muir, D.C. and P.H. Howard, Are there other persistent organic pollutants? A challenge for environmental chemists. Environmental science & technology, 2006. 40(23): p. 7157-7166.

[6] Qu, X., P.J. Alvarez, and Q. Li, Applications of nanotechnology in water and wastewater treatment. Water research, 2013. 47(12): p. 3931-3946.

[7] Opher, T. and E. Friedler, Factors affecting highway runoff quality. Urban Water Journal, 2010. 7(3): p. 155-172.

[8] Yan, A., et al., Solvothermal synthesis and characterization of size-controlled Fe 3 O 4 nanoparticles. Journal of Alloys and Compounds, 2008. 458(1): p. 487-491.

[9] Wakeman, R. and C. Williams, Additional techniques to improve microfiltration. Separation and Purification Technology, 2002. 26(1): p. 3-18.

[10] Mateen, F., et al., New method for the adsorption of organic pollutants using natural zeolite incinerator ash (ZIA) and its application as an environmentally friendly and cost-effective adsorbent. Desalination and Water Treatment, 2015(ahead-of-print): p. 1-9.

[11] Adelodun, A.A., Y.H. Lim, and Y.M. Jo, Surface oxidation of activated carbon pellets by hydrogen peroxide for preparation of CO 2 adsorbent. Journal of Industrial and Engineering Chemistry, 2014. 20(4): p. 2130-2137.

[12] Patnaik, P., Handbook of environmental analysis: chemical pollutants in air, water, soil, and solid wastes2010: CRC Press.

[13] Zhan, Y., et al., A novel carbon nanotubes/Fe 3 O 4 inorganic hybrid material: synthesis, characterization and microwave electromagnetic properties. Journal of magnetism and magnetic materials, 2011. 323(7): p. 1006-1010.

[14] Ayala, P., et al., The doping of carbon nanotubes with nitrogen and their potential applications. Carbon, 2010. 48(3): p. 575-586.

[15] Fatima, T., et al., Sorption of lead by chemically modified rice bran. International Journal of Environmental Science and Technology, 2013. 10(6): p. 1255-1264.

[16] Mastral, A., et al., PAH mixture removal from hot gas by porous carbons. From model compounds to real conditions. Industrial & Engineering Chemistry Research, 2003. 42(21): p. 5280-5286.

[17] Dharmambal, S., N. Mani, and D. Kannan, Adsorption of Rhodamine-B Dye from the aqueous Solution by using Tectonagrandis Bark Powder. Asian Journal of Research in Chemistry, 2015. 8(5): p. 346.

[18] Lasheen, M.R., N.S. Ammar, and H.S. Ibrahim, Adsorption/desorption of Cd (II), Cu (II) and Pb (II) using chemically modified orange peel: Equilibrium and kinetic studies. Solid State Sciences, 2012. 14(2): p. 202-210.

[19] AjayKumar, A.V., N.A. Darwish, and N. Hilal, Study of various parameters in the biosorption of heavy metals on activated sludge. World Applied Sciences Journal, 2009. 5(5).

[20] Ismail, M.G.B.H., et al., Freundlich Isotherm Equilibrium Equastions in Determining Effectiveness a Low Cost Absorbent to Heavy Metal Removal In Wastewater (Leachate) At Teluk Kitang Landfill, Pengkalan Chepa, Kelantan, Malaysia. Journal of Geography and Earth Science, 2013. 1(1): p. 01-08.

[21] Ahmaruzzaman, M., A review on the utilization of fly ash. Progress in Energy and Combustion Science, 2010. 36(3): p. 327-363.

[22] Pandey, R., et al., Fluorescent zinc (II) complex exhibiting “on-off-on” switching toward Cu2+ and Ag+ ions. Inorganic chemistry, 2011. 50(8): p. 3189-3197.

[23] Ramana, D.V., J.S. Yu, and K. Seshaiah, Silver nanoparticles deposited multiwalled carbon nanotubes for removal of Cu (II) and Cd (II) from water: Surface, kinetic, equilibrium, and thermal adsorption properties. Chemical Engineering Journal, 2013. 223: p. 806-815.